Li-Hsin Han

Wei Wang

Department of Mechanical Engineering,
University of Texas at Austin,
Austin, TX 78712

Yalin Lu

R. J. Knize

Physics Department,
Laser Optics Research Center,
USAF Academy,
Colorado Springs, CO 80840

Kitt Reinhardt
AFOSR/NE,
875 North Randolph Street, Suite 326,
Arlington, VA 22203

John Howell

Shaochen Chen[1]
e-mail: scchen@mail.utexas.edu

Department of Mechanical Engineering,
University of Texas at Austin,
Austin, TX 78712

Analytical and Experimental Investigations of Electromagnetic Field Enhancement Among Nanospheres With Varying Spacing

A modified Mie scattering theory was used to calculate the enhancement of electromagnetic (EM) field between gold nanospheres. The simulation result showed that the density of EM-energy in the space between neighboring nanospheres increases drastically as the interparticle space decreases. Simulated absorption-spectra also showed a peak-shifting from the visible to the infrared region when decreasing the nanosphere spacing. We used our previous experiment to verify the analytical results; the experiment was conducted by using a photodeformable microshell, which was coated with gold nanospheres. Made of photoshrinkable azobenzene polyelectrolytes, the microshells supported the gold nanospheres and gave the tunability of the interparticle spacing among the nanospheres. Upon irradiation of ultraviolet light, the microshells shrank and reduced the interparticle space. The absorption-spectra of the gradually shrinking microshells showed significant changes; a peak-broadening from the visible to the near-infrared region and a drastically enhanced water-absorption were observed in the experimental spectra. The experimental results confirmed the analytical analysis based on the modified scattering theory.
[DOI: 10.1115/1.3056574]

1 Introduction

Since the beginning of the last century, Mie scattering theory has become a very useful tool to analyze the enhancement of electromagnetic-wave by small particles [1,2]. Mie theory gives an exact solution to the distribution of electromagnetic field around one isolated, homogeneous, spherical object under the irradiation of a plane-wave. The solution successfully predicted the existence of multiple resonances, at which the scattering and absorption of the incident light by the sphere are maximized at specific wavelengths. In addition to conventional optics, the Mie scattering theory has brought important insight to many fields. For example, the electromagnetic resonance also induces a resonance of surface-electrons, which may trigger chemical reactions. For the case of metallic spheres for photocatalysis [3], the Mie theory was generally used to explain the formation of photo-electrons, which are responsible for the photochemical effects. Moreover, the Mie scattering theory was used for the study of photonic crystals [4] and photovoltaic devices [5].

For problems involving multiple-spheres, the original Mie model could lead to an approximated solution. The accuracy of the approximation, however, depends on the significance of the scattering effect among spheres, in which the light scattered by each sphere irradiates the whole system and becomes a part of the incident light. The intensity of multiple-scattering depends strongly on interparticle spacing. When the spacing is sufficiently large, the multiple-scattering effect becomes negligible and the scattering and absorption by the whole system are close to the linear combination of Mie's original solution for each individual sphere. In many real experiments, however, the particles are so concentrated that the multiple-scattering effect becomes important, and the linear combination approach becomes questionable. To solve the multiple-sphere problem, a modified Mie model was proposed decades ago to cover the multiple-scattering effects [6]. This modified theory differs from the original one by adding the scattering from each sphere $\vec{E}_s^i$ (which is unknown) to the incident wave. This model offers an exact solution for a multiple-sphere system, where the sphere size and optical property can be different from one to another. In the beginning, the application of this model was quite limited due to low computer-capacity [6]. In recent years, it has become possible to apply this model to a system of thousands of spheres. Surprisingly, however, little attention was paid to applying the modified Mie theory to real experiments that involve concentrated spheres. In this paper, we use the modified Mie scattering theory to simulate the electromagnetic-field enhancement by two gold nanospheres of varying spacing. We also develop an experiment to verify the simulation results. In the experiment, a photodeformable microshell coated with gold nanospheres is used to form a multiple-sphere-medium of tunable spacing. Upon irradiation with ultraviolet light, the microshells shrink gradually, leading to the decrease in the nanosphere spacing. The absorption-spectra of the microshells are measured to compare the simulation results.

[1]Corresponding author.
Contributed by the Heat Transfer Division of ASME for publication in the JOURNAL OF HEAT TRANSFER. Manuscript received July 11, 2008; final manuscript received October 7, 2008; published online January 23, 2009. Review conducted by Robert D. Tzou. Paper presented at the 2008 International Conference on Micro/Nanoscale Heat Transfer (MNHT2008), Tainan, Taiwan, January 6–9, 2008.

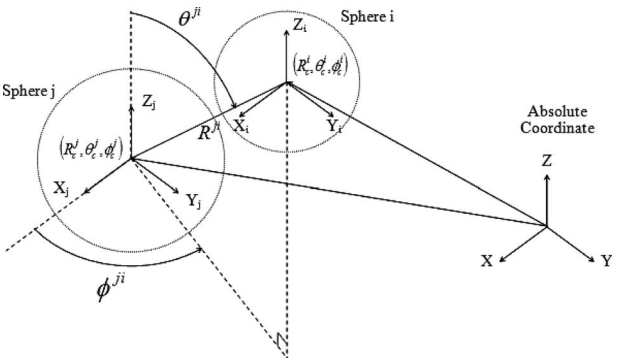

Fig. 1 A coordinate-system for the multiple-spheres. $(R^{ji}, \theta^{ji}, \phi^{ji})$ denotes the central point of sphere *i* with respect to the center of sphere *j*.

2 Analytical Analysis of the Electromagnetic Field in a Multisphere System

In the modified Mie theory, the electric field in the system $\vec{E}_{\text{total}}$ consists of the incident plane-wave $\vec{E}_0$ and the scattering by all particles $\vec{E}_s$, where $\vec{E}_s=\Sigma_{i=1}^{Ns}\vec{E}_s^i$. For linearization, the incident field $\vec{E}_i$ (typically a plane-wave), scattered field $\vec{E}_s$, and internal field $\vec{E}_1^i$ (the field inside a sphere) are expanded into polynomials of orthogonal vectors $\vec{M}_{mn}^{(j)}$ and $\vec{N}_{mn}^{(j)}$ as follows:

$$\vec{E}_0=\sum_{n=1}^{\infty}\sum_{m=-n}^{n}[p_{mn}\vec{N}_{mn}^{(1)}(r,\theta,\phi)+q_{mn}\vec{M}_{mn}^{(1)}(r,\theta,\phi)] \tag{1}$$

$$\vec{E}_s=\sum_{i=1}^{N_s}\sum_{n=1}^{\infty}\sum_{m=-n}^{n}[a_{mn}^i\vec{N}_{mn}^{(3)}(r^i,\theta^i,\phi^i)+b_{mn}^i\vec{M}_{mn}^{(3)}(r^i,\theta^i,\phi^i)]|_{R^i>a^i} \tag{2}$$

$$\vec{E}_1^i=\sum_{n=1}^{\infty}\sum_{m=-n}^{n}[d_{mn}^i\vec{N}_{mn}^{(1)}(m^ir^i,\theta^i,\phi^i)+c_{mn}^i\vec{M}_{mn}^{(1)}(m^ir^i,\theta^i,\phi^i)]|_{R^i<=a^i} \tag{3}$$

The derivation of these orthogonal vectors was given in Ref. [6]. Figure 1 illustrates the coordinate-system for the multiple-sphere problem. The spheres are numbered from 1 to N_s. The orthogonal vectors are calculated from $\vec{M}_{mn}^{(j)}=\nabla\times\vec{R}u_{mn}^{(j)}$ and $\vec{N}_{mn}^{(j)}=(1/k)\nabla\times M_{mn}^{(j)}$. $\vec{R}=(R,\theta,\phi)$ is a position with respect to the origin of a spherical coordinate-system. The r in the equations is a dimensionless radius derived from R, and $r=k\cdot R$, where k is the wave constant of the incident light in the surrounding media. (r^i,θ^i,ϕ^i) is the relative position with respect to the center of sphere i. $u_{mn}^{(j)}$ is the spherical harmonic function, where $u_{mn}^{(1)}=j_n(r)P_n^m(\cos\theta)e^{im\phi}$ and $u_{mn}^{(3)}=h_n(r)P_n^m(\cos\theta)e^{im\phi}$. P_n^m is a term of associated Legendre polynomial, $j_n(r)$ is the nth order spherical Bessel function, and $h_n(r)$ is the nth order spherical Hankel functions. a^i in Eq. (2) is the radius of sphere i. m^i in Eq. (3) is the relative dielectric constant of sphere i, $m^i=\sqrt{\varepsilon_s^i/\varepsilon_m}$.

To calculate the distribution of the electromagnetic field, we need to find the expansion coefficients p_{mn}, q_{mn}, c_{mn}^i, d_{mn}^i, a_{mn}^i, and b_{mn}^i. First, we need to transfer the origin of Eq. (1) to the center of each sphere i

$$\vec{E}_0=\sum_{n=1}^{\infty}\sum_{m=-n}^{n}[p_{mn}^i\vec{N}_{mn}^{(1)}(r^i,\theta^i,\phi^i)+q_{mn}^i\vec{M}_{mn}^{(1)}(r^i,\theta^i,\phi^i)] \tag{4}$$

For convenience, the direction of the electric field of the incident plane-wave $\vec{E}_0$ is set to be parallel to the x-direction of the absolute coordinate-system (see Fig. 1) and the wave vector $\vec{k}$ is parallel to the z-direction. That is, $\vec{E}_0=\hat{x}E_0\exp(ikR^0\cos\theta^0)$. Note that we denoted (R^0,θ^0,ϕ^0) as the absolute position in the space. With respect to the center of sphere i, $(R_c^i,\theta_c^i,\phi_c^i)$, the theory gives $p_{1n}^i=-\frac{1}{2}i^{n+1}E_0((2n+1)/n(n+1))\exp(ikR_c^i\cos\theta_c^i)$, $p_{-1n}^i=\frac{1}{2}i^{n+1}E_0(2n+1)\exp(ikR_c^i\cos\theta_c^i)$, $q_{1n}^i=p_{1n}^i$, $q_{-1n}^i=-p_{-1n}^i$, and $q_{mn}^i=p_{mn}^i=0$ for $|m|\neq 1$.

To calculate coefficients a_{mn}^i and b_{mn}^i, we use the continuity boundary condition at the surface of each sphere [7]. The tangential components of electric and magnetic fields are continuous across the boundary of the surface of each sphere

$$\left(\vec{E}_0+\sum_{i=1}^{N_s}\vec{E}_s^i-\vec{E}_1^i\right)\times\hat{e}_r|_{R^i=a^i}=0 \tag{5}$$

$$\left(\vec{H}_0+\sum_{i=1}^{N_s}\vec{H}_s^i-\vec{H}_1^i\right)\times\hat{e}_r|_{R^i=a^i}=0 \tag{6}$$

To solve a_{mn}^i and b_{mn}^i linearly, we need two more equations to relate the expansion vectors of sphere i, $\vec{N}_{mn}^{(1,3)}(r^i,\theta^i,\phi^i)$ and $\vec{M}_{mn}^{(1,3)}(r^i,\theta^i,\phi^i)$, to the expansion vectors of a different sphere j, $\vec{N}_{mn}^{(1,3)}(r^j,\theta^j,\phi^j)$ and $\vec{M}_{mn}^{(1,3)}(r^j,\theta^j,\phi^j)$,

$$\vec{M}_{mn}^{(3)}(r^j,\theta^j,\phi^j)=\sum_{l=1}^{\infty}\sum_{k=-l}^{l}[A_{kl}^{mn}(r^{ji},\theta^{ji},\phi^{ji})\vec{M}_{kl}^{(1)}(r^i,\theta^i,\phi^i)+B_{kl}^{mn}(r^{ji},\theta^{ji},\phi^{ji})\vec{N}_{kl}^{(1)}(r^i,\theta^i,\phi^i)] \tag{7}$$

$$\vec{N}_{mn}^{(3)}(r^j,\theta^j,\phi^j)=\sum_{l=1}^{\infty}\sum_{k=-l}^{l}[A_{kl}^{mn}(r^{ji},\theta^{ji},\phi^{ji})\vec{N}_{kl}^{(1)}(r^i,\theta^i,\phi^i)+B_{kl}^{mn}(r^{ji},\theta^{ji},\phi^{ji})\vec{M}_{kl}^{(1)}(r^i,\theta^i,\phi^i)] \tag{8}$$

$(r^{ji},\theta^{ji},\phi^{ji})$ denotes the center of sphere i with respect to the center of sphere j. The calculations of $A_{kl}^{mn}(r^{ji},\theta^{ji},\phi^{ji})$ and $B_{kl}^{mn}(r^{ji},\theta^{ji},\phi^{ji})$ are given by Ref. [6]. Combining Eqs. (1)–(8) we get the linear equations for all a_{mn}^i and b_{mn}^i as follows:

$$\begin{pmatrix}a_{mn}^i\\ b_{mn}^i\end{pmatrix}=\begin{pmatrix}-\alpha_n^ip_{mn}^i\\ -\beta_n^iq_{mn}^i\end{pmatrix}+\begin{pmatrix}-\alpha_n^iA_{mn}^{kl}(r^{ji},\theta^{ji},\phi^{ji}) & -\alpha_n^iB_{mn}^{kl}(r^{ji},\theta^{ji},\phi^{ji})\\ -\beta_n^iB_{mn}^{kl}(r^{ji},\theta^{ji},\phi^{ji}) & -\beta_n^iA_{mn}^{kl}(r^{ji},\theta^{ji},\phi^{ji})\end{pmatrix}\times\begin{pmatrix}a_{kl}^j\\ b_{kl}^j\end{pmatrix} \tag{9}$$

The coefficients α_n^i and β_n^i are given as

$$\alpha_n^i=\frac{m^i\psi_n'(x^i)\psi_n(m^ix^i)-\psi_n(x^i)\psi_n'(m^ix^i)}{m^i\xi_n'(x^i)\psi_n(m^ix^i)-\xi_n(x^i)\psi_n'(m^ix^i)} \tag{10}$$

$$\beta_n^i=\frac{\psi_n'(x^i)\psi_n(m^ix^i)-m^i\psi_n(x^i)\psi_n'(m^ix^i)}{\xi_n'(x^i)\psi_n(m^ix^i)-m^i\xi_n(x^i)\psi_n'(m^ix^i)} \tag{11}$$

where $x^i=ka^i$, $\psi_n(\rho)=\rho j_n(\rho)$, and $\xi_n(\rho)=\rho h_n(\rho)$. The primes in Eqs. (10) and (11) denote the differentiations with respect to arguments.

The expansion coefficients for the internal field of sphere, c_{mn}^i, and d_{mn}^i, are calculated by using boundary conditions (5) and (6). We get

$$c^i_{mn} = \frac{\mathrm{i}m^i}{\psi'_n(x^i)\psi_n(m^i x^i) - m^i\psi_n(x^i)\psi'_n(m^i x^i)} b^i_{mn} \tag{12}$$

$$d^i_{mn} = \frac{\mathrm{i}m^i}{m^i\psi'_n(x^i)\psi_n(m^i x^i) - \psi_n(x^i)\psi'_n(m^i x^i)} a^i_{mn} \tag{13}$$

Important properties of the multiple-sphere system are calculated by using the expansion coefficients. For example, the energy absorption (unit: Watt) by sphere i is

$$W^i_{\mathrm{abs}} = \frac{1}{2}\mathrm{Re}\left\{\int_{A(r^i=x^i)} (\vec{E}^i_1 \times \vec{H}^i_1)\cdot(-\hat{e}_r)\right\}$$
$$= \frac{2\pi E_0^2}{|m^i|^2\omega}\sum_{n=1}^{\infty}\sum_{m=-n}^{n}\frac{n(n+1)(n+m)!}{(2n+1)(n-m)!}\mathrm{Re}\left\{\frac{\mathrm{i}}{k\mu}\psi'_n(m^i x^i)\psi^*_n(m^i x^i)\right.$$
$$\left.\times(m^{i*}|d_{mn}|^2 + m^i|c_{mn}|^2)\right\} \tag{14}$$

where * denotes a complex conjugate. Similarly, the energy extinction (the separated energy from the original, incident flow of light) by sphere i is

$$W^i_{\mathrm{ext}} = \frac{1}{2}\mathrm{Re}\left\{\oint_{A(r^i=x^i)} (\vec{E}^i_0 \times \vec{H}^i_s + \vec{E}^i_s \times \vec{H}^i_0)\cdot(-\hat{e}_r)\right\}$$
$$= \frac{2\pi E_0^2}{\omega}\sum_{n=1}^{\infty}\sum_{m=-n}^{n}\frac{n(n+1)(n+m)!}{(2n+1)(n-m)!}\mathrm{Re}\left\{\frac{\mathrm{i}}{k\mu}(a^i_{mn}p^{i*}_{mn} + b^i_{mn}q^{i*}_{mn})\right.$$
$$\left.\times(\psi^*_n(x^i)\xi'_n(x^i) - \psi'^*_n(x^i)\xi_n(x^i))\right\} \tag{15}$$

The energy scattered by sphere i is simply the difference between W^i_{abs} and W^i_{ext},

$$W^i_{\mathrm{sca}} = W^i_{\mathrm{ext}} - W^i_{\mathrm{abs}} \tag{16}$$

The energy flux I_i (unit: $\mathrm{W/m^2}$) of the incident wave equals $(E_0^2/2\omega)\cdot\mathrm{Re}\{k/\mu\}$. Three constantly used properties [7], the absorption, extinction, and scattering cross sections (unit: $\mathrm{m^2}$), are given by $C^i_{\mathrm{abs}} = W^i_{\mathrm{abs}}/I_i$, $C^i_{\mathrm{ext}} = W^i_{\mathrm{ext}}/I_i$, and $C^i_{\mathrm{sca}} = W^i_{\mathrm{sca}}/I_i$.

The number n for a^i_{mn} and b^i_{mn} expands from 1 to infinity. Technically, the solution for Eqs. (1)–(3) will be sufficiently precise at a certain order N ($n=1,2,\ldots,N$). In general, a larger N is needed to solve a problem of closer spheres [8].

3 Modeling the Interaction Between Two Gold Nanospheres Under Irradiation

We study the multiple-scattering effect between two gold nanospheres by using the modified Mie theory. We used two kinds of medium dielectric constant ε_m to study the enhancement of electromagnetic field outside the spheres. Reference [9] was used for the dielectric constant ε_m of water, and $\varepsilon_m=1$ was used for vacuum. The diameter of each gold sphere is 40 nm. The dielectric constant of the bulk-material of gold, $\varepsilon_{s,\mathrm{bulk}}$, is from Ref. [10]. Because the size of a 40 nm gold sphere is comparable to the mean-free-path of electrons in a gold bulk-material [11], modification terms are needed to cover the damping effect from the confinement of electrons by the particle surface [12],

$$\varepsilon_s = \varepsilon_{s,\mathrm{bulk}} + \frac{\omega_p^2}{\omega^2 + i\gamma_{\mathrm{bulk}}\omega} - \frac{\omega_p^2}{\omega^2 + i\gamma\omega} \tag{19}$$

where $\gamma = \gamma_{\mathrm{bulk}} + Av_f/a$. a is the sphere radius. A is a constant normally assigned 1. For a gold bulk-material, the damping constant γ_{bulk} is 1.1×10^{14} Hz, the plasma frequency ω_p is 1.37×10^{16} Hz [13], and the Fermi velocity v_f equals 1.39×10^6 m/s [14].

The order N of the linear equation was carefully selected to make sure that the error of the calculated absorption by the spheres is less than 1%.

The spheres are both positioned at the X-axis and are aligned parallel to the incident electric field. Different interparticle spaces were used in our simulation: 10 nm, 5 nm, 1 nm, and 0.1 nm. Figure 2 shows the field enhancement at the X-Y plane of our bispherical system irradiated by 700 nm light in vacuum environment. The energy density I ($\mathrm{W/m^3}$) was calculated according to $I=\frac{1}{4}(\vec{E}\cdot\vec{D}+\vec{B}\cdot\vec{H})$ [7]. The plot illustrates the intensity ratio of the enhanced field to the incident light. The result shows that the field-intensity at the mass-center of the two spheres grows sharply and nonlinearly as the spheres become closer. In the case of 0.1 nm spacing, as shown by Fig. 2(d), the intensity grows more than 10^5-fold compared with the incident plane-wave.

Figure 3 shows the spectrum of absorption cross section of the bispherical system (in vacuum) of different interparticle spaces. For comparison, the same figure also shows the spectrum of an isolated sphere. When the interparticle space is large (10 nm and beyond), the spectrum is very close to double that of the isolated-particle spectrum, because there is no significant coupling between the scatterings of the two spheres. As the spheres become closer to each other, the multiple-scattering effect raises the total absorption. Note that the absorption-peak of the bispherical system undergoes a major redshift as the spheres approach each other. This redshifting shows the interaction between the two spheres through their scattering field. A simple yet effective model that explains the forming of this spectrum-shifting by a nanoparticle pair is given in Ref. [15]. In brief, when two particles are aligned parallel to the incident electric field, the electric dipoles formed at each sphere interact and delay the response to the incident field. The delay causes the redshifting at the system's resonance frequency.

Figure 4 shows the simulation result about the bispherical system in a water medium. The results show a strong enhancement of absorption by water in the gap between the two spheres. Figures 4(a) and 4(b) show the absorption spectrum of water ($\mathrm{W/m^3}$) at the center of the gap. Figure 4(b) is the logarithmic plot of Fig. 4(a). The water-absorption is increased over 1000-fold when the interparticle spacing changes from 10 nm to 0.1 nm. The enhancement of the finger-print absorption-peak for water at 970 nm is clearly seen in the simulation result. The trapping of high-density photo-energy in the space between close spheres, as shown in Fig. 2(d), explains the enhanced water-absorption. This simulation was later compared with the result of the experiment using our nanoparticle-coated, photodeformable microshells. The effect of quantum confinement may become important when the interparticle spacing is very small. For simplicity, we only focus on using the modified Mie's theory and show the trend of surface plasmon enhancement in a classical approach. In a real case, however, the interparticle spacing may become no smaller than 1 nm due to the space taken by surface ligands (citric acid) on the Au nanoparticles.

4 Experiment

To experimentally demonstrate the near-field enhancement among nanospheres, in a previous study [17], we fabricated microshells using a photosensitive polymer. These microshells shrink upon the irradiation by ultraviolet (UV) light. We coated the surface of the microshells with 40 nm gold nanospheres. Upon UV irradiation, the microshell shrank and the shrinkage reduces the interparticle spaces of the nanospheres on the surface. The spectrum of the microshells was taken to study the change in absorption during different stages of shrinking. The microshell contains a chemical called azobenzene (AZO). Azobenzene undergoes a *trans*-to-*cis* isomerization [16] (at which the molecule atoms realign without changing the original connections) by absorbing UV light. An isomerized azobenzene molecule reduces its

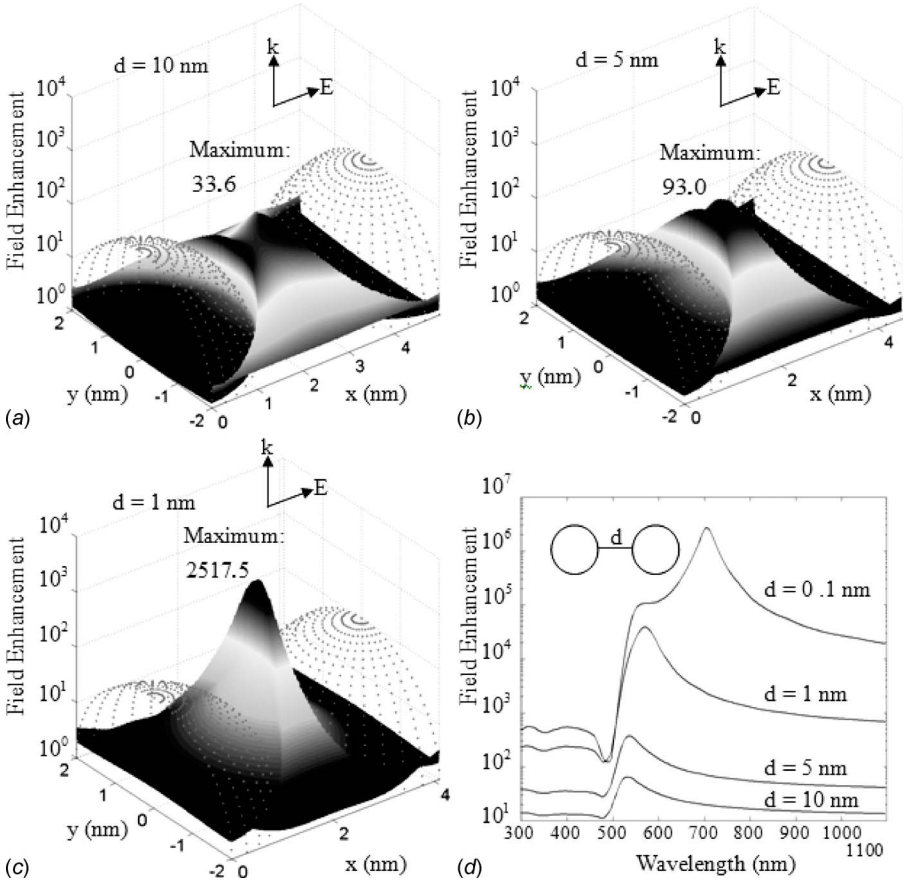

Fig. 2 The simulated enhancement of energy density between two close spheres in vacuum. (*a*)–(*c*) illustrate the intensity ratio of the enhanced field to the incident light; the wavelength is 700 nm in these plots and the interparticle spaces in the plots are (*a*) 10 nm, (*b*) 5 nm, and (*c*) 1 nm. (*d*) shows the spectra of field-enhancement at the center of different gaps, from 10 nm to 0.1 nm.

length from approximately 0.9 nm to 0.55 nm and converts light directly to mechanical deformation. Details about the fabrication of the microshells are given in Ref. [17]. In brief, the AZO-contained polymer was coated onto the surface of a 6 μm silica microsphere through electrostatic adhesion in water environment. After electrostatically coating the 40 nm Au nanospheres onto the polymer layer, the silica core was etched away by buffered hydrofluoric (BHF) acid. The structure of the nanosphere-coated shell remains intact during the etching.

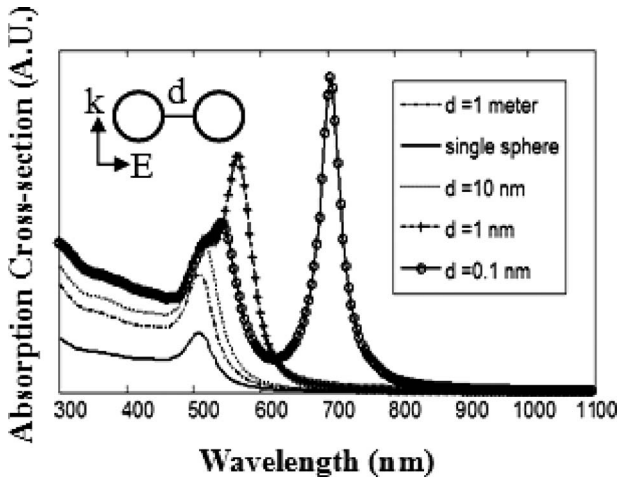

Fig. 3 The simulated absorption-spectra of the bispherical system of different gaps. The medium is vacuum. The absorption spectrum of a single particle is included for comparison.

A scanning electron microscopy (SEM) picture (Fig. 5(*a*)) of the microshell before the removal of the silica core shows the initial interparticle spaces among nanospheres (inset of Fig. 5(*a*)). Most of the gaps were comparable to the sphere diameter (40 nm), while a few nanospheres were originally in contact. The microshells, which collapse when dried (Fig. 5(*b*)), were turgid and slightly swelled in water (Fig. 5(*c*)). The shell diameter was approximately 6.2 μm. Upon UV irradiation, the microshells gradually shrank to a final size of 4.0 μm (Fig. 5(*d*)). The number of contacting nanospheres grew after the shrinkage.

Figure 6(*a*) shows the change in absorption spectrum of the microshells. Our experiment shows a dramatic rise in the near-infrared (NIR) region and a drop in the peak around 560 nm, which is close to the absorption-peak (~530 nm) of the gold nanosphere (Fig. 6(*b*)). This change indicates a redshift of absorption by the nanospheres. Because the distribution of Au nanospheres was random, the peak-shifting from our simulation is unobservable in the experimental result. Instead, we observed a broadening from the original 560 nm peak toward the NIR region. In our previous study [17], we compared this effect with a controlled experiment using the photoshrinkable microshells of no Au nanoparticles. Upon UV irradiation, the blank microshells show a slight spectrum change, which came from the photo-isomerization of the AZO-group and also by the change in molecule concentration during shrinking. The change in control spectrum, however, was negligible compared with the change in Fig. 6(*a*).

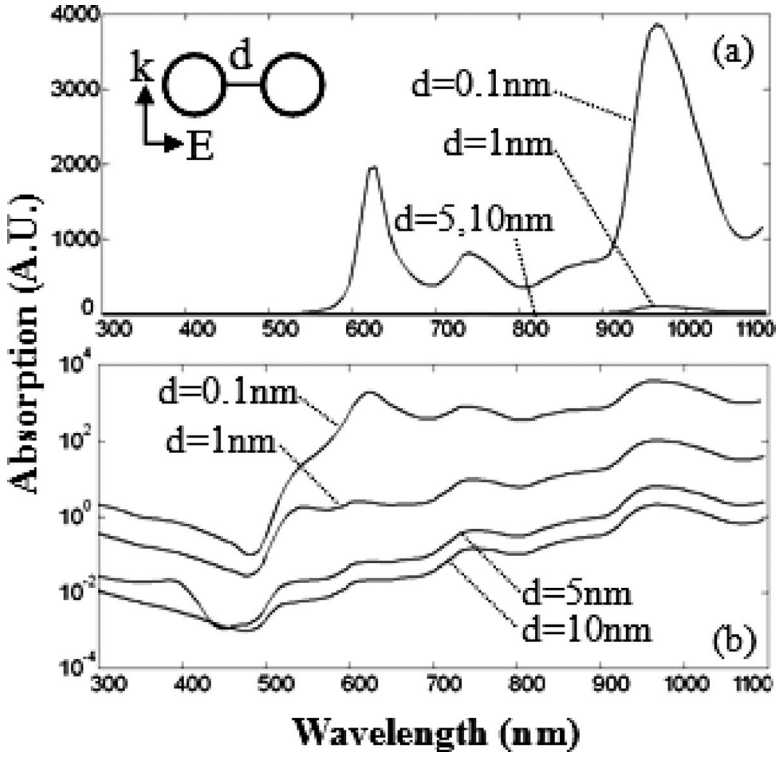

Fig. 4 (*a*) **The spectra of water at the center of different particle gaps. Note the rising peak at 970 nm, which indicates the enhancement of water-absorption. This change was observed in our experiment.** (*b*) **A logarithmic plot of** (*a*)**.**

Importantly, these experimental results confirmed the effect of field-enhancement, which stems from the interaction among neighboring nanospheres. The spectra show that the enhanced NIR absorption has another source, in addition to the nanosphere interactions. The increasing peak at 970 nm, which is from the second overtune frequency of water molecule [18], indicates a significantly increased absorption of water. Compared with the original 970 nm peak of the spectrum of nonirradiated microshells, the absorption of water in the NIR region was increased more than 100-fold. The enhanced water-absorption confirmed that a strong field-enhancement had taken place due to the shrinkage of microshells, as shown by our simulation shown in Fig. 4.

5 Conclusion

We used a modified Mie scattering theory to calculate the exact solutions for a bispherical system of a changing interparticle

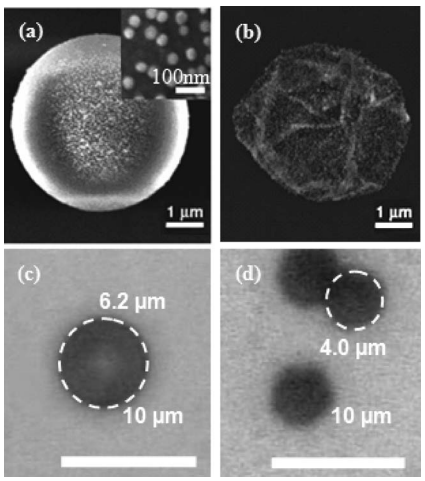

Fig. 5 The photodeformable microshell(s). (*a*) **The SEM picture of one microshell before the removal of its silica core. The inset shows a close look at the surface nanospheres.** (*b*) **The SEM picture of a dried, collapsed microshell.** (*c*) **A nonirradiated microshell in water, under an optical microscope.** (*d*) **Microshells after the irradiation by UV light. The shell-diameters reduced about 35%.**

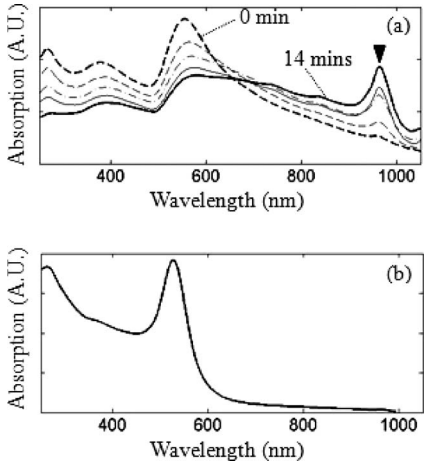

Fig. 6 (*a*) **The experimental spectra of the microshells under different stages of irradiation, from 0 min to 14 min. The triangle indicates the raising peak of water-absorption at 970 nm. The broadening of absorption-peak at 560 nm indicates the change in particle-interaction during the shell-shrinking, as shown by the simulation.** (*b*) **The spectrum of diluted 40 nm gold nanospheres in water. This figure is used to compare with the spectra of** (*a*)**.**

space. Based on the simulation results, we showed that a redshift in gold-sphere absorption and a significant field-enhancement in the sphere-gap would take place when the interparticle space approaches zero. The theoretical result was confirmed by a previous experiment using our nanosphere-coated, photodeformable microshells. We show that the modified Mie model is an effective tool for solving the multiple-scattering problem. This article also sheds light on the application of electromagnetic-interaction between small particles to different research fields, such as photonics, photochemistry, and probably photovoltaic materials.

Acknowledgment

This work was partially supported by grants from the U.S. National Science Foundation, Office of Naval Research, and the Air Force Office of Scientific Research. We thank Professor Stephen E. Webber in the Department of Chemistry and Biochemistry at UT-Austin for equipment support.

References

[1] Mie, G., 1908, "Beiträge zur Optik trüber Medien speziell kolloidaler Metallösungen," Ann. Phys., **25**, pp. 376–445.
[2] Craig, F. B., and Donld, R. H., 1983, *Absorption and Scattering of Light by Small Particles*, Wiley, Canada, pp. 83–129.
[3] Shvalagin, V. V., Stroyuk, A. L., and Kuchmii, S. Y., 2007, "Photochemical Synthesis of ZnO/Ag Nanocomposites," J. Nanopart. Res., **9**(3), pp. 427–440.
[4] Vandenbem, C., and Vigneron, J. P., 2005, "Mie Resonances of Dielectric Spheres in Face-Centered Cubic Photonic Crystals," J. Opt. Soc. Am. A, **22**(6), pp. 1042–1047.
[5] Banerjee, M., Datta, S. K., and Saha, H., 2005, "Enhanced Optical Absorption in a Thin Silicon Layer With Nanovoids," Nanotechnology, **16**(9), pp. 1542–1548.
[6] Mackowski, D. W., 1991, "Analysis of Radiative Scattering for Multiple Sphere Configurations," Proc. R. Soc. London, Ser. A, **433**, pp. 599–614.
[7] Jackson, J. D., 1999, *Classical Electrodynamics*, 3rd ed., Wiley, New York, pp. 352–356.
[8] Chern, R., Liu, X., and Chang, C., 2007, "Particle Plasmons of Metal Nanospheres: Application of Multiple Scattering Approach," Phys. Rev. E, **76**, p. 016609.
[9] Segelstein, D., 1981, "The Complex Refractive Index of Water," MS thesis, University of Missouri, Kansas City, MO.
[10] Weaver, J. H., and Frederikse, H. P. R., 2001, *Optical Properties of Selected Elements*, 82nd ed., CRC, Boca Raton, FL.
[11] Kreibig, U., and Vollmer, M., 1995, *Optical Properties of Metal Clusters*, Springer, New York.
[12] Kawata, S., 2001, *Near-Field Optics and Surface Plasmon Polaritons*, Springer, New York.
[13] Johnson, P. B., and Christy, R. W., 1972, "Optical Constants of the Noble Metals," Phys. Rev. B, **6**, pp. 4370–4379.
[14] Kittel, C., 1971, *Introduction to Solid State Physics*, 4th ed., Wiley, Canada, p. 248.
[15] Rechberger, W., Hohenau, A., Leitner, A., Krenn, J. R., Lamprecht, B., and Aussenegg, F. R., 2003, "Optical Properties of Two Interacting Gold Nanoparticles," Opt. Commun., **220**, pp. 137–141.
[16] Feringa, B. L., 2001, *Molecular Switches*, Wiley-VCH, Weinheim, p. 399.
[17] Han, L., Tang, T., and Chen, S., 2006, "Tuning the Absorptions of Au Nanospheres on a Microshell by Photo-Deformation," Nanotechnology, **17**, pp. 4600–4605.
[18] Palmer, K. F., and Williams, D., 1974, "Optical Properties of Water in the Near Infrared," J. Opt. Soc. Am., **64**(8), pp. 1107–1110.